High-accuracy mapping of inundations induced by ice jams: a case study from Iceland

Emmanuel Pagneux and Árni Snorrason

ABSTRACT

Hydraulic modelling is widely used for deriving flood hazard maps featuring depth of flooding and flow velocity from discharge scenarios. Due to uncertainties about flow conditions or inaccurate terrain models, flood hazards maps obtained from hydraulic modelling may be of limited relevance and accuracy. Hydraulic modelling is particularly challenging in Arctic regions, where ice jams lead to flooding in areas that would not be subjected to inundation under open-water conditions. As numerical models of ice jam processes require information that may be difficult and expensive to collect, an alternative approach based on the photo interpretation of documented historical events is presented here. Orthophotographs and a digital elevation model at high resolution are used to support the photo interpretation process. Tested in an Icelandic watershed prone to ice jam floods, reconstructions provide locally unprecedented and robust information on the extent and depth of flooding of inundations induced by ice jams.

Key words | 3D analysis, flood hazard mapping, ice jam flood, Iceland, photo interpretation, spatial analysis

Emmanuel Pagneux (corresponding author)
Icelandic Meteorological Office,
Bústaðavegur 9,
150 Reykjavík,
Iceland
Department of Geography and Tourism,
Faculty of Life and Environmental Sciences,
University of Iceland,
101 Reykjavík,
Iceland
E-mail: *emmanuel@vedur.is*

Árni Snorrason
Icelandic Meteorological Office,
Bústaðavegur 9,
150 Reykjavík,
Iceland

INTRODUCTION

Depth of flooding and flow velocity are flood hazard parameters of particular concern regarding the safety of structures, the safety of people, and the emergency response. The impact of flow velocity is, for instance, particularly strong on road infrastructures (Kreibich *et al*. 2009). Hydrostatic action imparted by water depth and capillarity rise have a strong impact on buildings (Kelman & Spence 2004), but a medium impact on road infrastructure; depth of flooding has a direct impact on the buoyancy of vehicles and therefore on the efficiency of the emergency response (MATE/METL 1999). As a result, flow velocity and depth of flooding are widely used in the production of flood hazard maps, which typically display visual information on the magnitude and likelihood of a flooding event, and of flood risk maps, which in turn emphasise the adverse consequences of flood hazards (Spachinger *et al*. 2008; de Moel *et al*. 2009). In the USA and Canada, flood mapping relies on the delineation of a base floodplain corresponding to a 100-year flood, and distinction is made in the base floodplain between the floodway, which includes the main channel and the adjacent overbank areas where water depths and flow velocities are the greatest, and the flood fringe, where depths and velocities are lower (Environment Canada 1993; NARA 2009). In countries where the European Directive on the Assessment and Management of Flood Risks applies (European Parliament and Council 2007), authorities are required to produce flood hazard maps that should include visual information on the inundation extent, depth of flooding and/or water levels, and flow velocity for discharge exceedance scenarios of low, medium, and high probabilities. A set of flood risk maps displaying visual information on the number of inhabitants and the type of activities affected, and on the 'installations which might cause accidental pollution', should also be produced. Finally, flood risk management plans should be developed accordingly. In many countries of Europe, classifications of areas prone to inundation have been established that rely on a combination of flood hazard parameters. In

doi: 10.2166/nh.2012.114

Table 1 | Flood hazard parameters and thresholds used for flood hazard classification in France (MATE/METL 1999)

Rating formula Depth of flooding (m)	Hazard rate (HR) = d × v, d = depth of flooding (m); v = velocity of floodwaters (m/sec) Velocity (m/s) <0.5	0.5–1	>1
<0.5	Low	Moderate	High
0.5–1	Moderate	Moderate	High
>1	High	High	Very high

France (Table 1) and in Austria, for instance, flood depths and flow velocities corresponding to a 100-year flood are combined to produce a danger-oriented classification of flood hazard (MATE/METL 1999; EXCIMAP 2007). In the UK (Table 2), harm potential of floating debris recruited during the onset of floods is taken into consideration in addition to flow velocity and depth of flooding to characterise the 100-year flood and the 1000-year flood (DEFRA 2006; DEFRA 2008). Restrictions in development and in land use planning may result directly from the classification of flood hazard. In France, development is strictly forbidden in areas where flood hazard is rated high or very high (French Parliament 1995; MATE/METL 1999) (Table 3). In contrast to the French approach, flood hazard rates produced in the UK have no binding effect on development (DCLG 2006).

Mapping of flooded areas according to discharge scenarios is typically obtained from hydraulic modelling (de Moel *et al.* 2009). Used as input parameter in hydraulic models (Bates & de Roo 2000), discharge is currently obtained from water levels observed using fitted rating curves (e.g. Moyeed & Clarke 2005), or derived from runoff coefficients in ungauged catchments (e.g. Merz *et al.* 2008). The use of hydraulic models for flood mapping purposes is, however, not self-evident. There are many factors affecting the accuracy of flood extent maps and flood depth maps obtained from hydraulic modelling, such uncertainties about flow conditions and friction coefficients, or inaccurate elevation models (Bales & Wagner 2009). In recent years, the use of high resolution digital elevation models (DEM) obtained from airborne laser altimetry or photogrammetric surveys has helped to produce flood maps of given discharge exceedance (e.g. Bales *et al.* 2007) and maps of historical flooding events of increased accuracy (e.g. Horrit *et al.* 2010). Hydraulic modelling is nonetheless challenging in Arctic regions, where ice jams lead to flooding in areas which at the same discharge would not be flooded under open-water conditions (Beltaos, 1995; Pagneux *et al.* 2010). Significant efforts have been devoted to numerical modelling of river ice processes over the past two decades (Beltaos 2008), with the development of one-dimensional models, e.g. ICEPRO (Carson *et al.* 2003) and of dynamic and two-dimensional models, e.g. CRISSP2D (Liu *et al.* 2006). All models have common parameters such as bathymetry, flow conditions, and jam location. Such information is not always available and is very expensive to collect. In the absence of information required for hydraulic modelling, the use of historical data and geomorphic evidence may provide a regulatory basis for the

Table 3 | Coercive flood risk zoning derived from flood hazard classification in France (MATE/METL 1999)

Flood hazard classification	Colour scheme	Flood risk zoning
Low, moderate	Blue	Development permitted under conditions (flood proofing)
High, very high	Red	Development not permitted

Table 2 | Flood hazard parameters and thresholds used for flood hazard classification in the UK (DEFRA 2006; 2008)

Rating formula	Hazard rate = d × (v + n) + DF, d = depth of flooding (m); v = velocity of floodwaters (m/sec); DF = debris factor (0, 0.5, 1 depending on probability that debris will lead to a hazard), n = a constant of 0.5	
Flood hazard rates	Colour scheme	Hazard to people classification
Less than 0.75	–	Very low hazard – caution
0.75 to 1.25	Yellow	Danger for some – includes children, the elderly and the infirm
1.25 to 2.0	Orange	Danger for most – includes the general public
More than 2.0	Red	Danger for all – includes the emergency services

delineation of floodplain in areas prone to ice jam floods. In the regulation of the Canadian province of Alberta, for instance, the design flood should correspond, in areas prone to ice jam floods, to a historical ice jam flooding event if a computed 100-year water level that would result from an ice jam cannot be obtained (Government of Alberta, http://environment.alberta.ca/01655.html); before the expiration in 1999 of the *Canada–Alberta Flood Damage Reduction Program*, the possibility of delineating ice hazard zones, defined as areas prone to damages from river ice movement, had been considered in addition to the federal floodway and flood fringe risk zones (Environment Canada 1993; Government of Alberta, http://www3.gov.ab.ca/env/water/flood/FDRP.pdf). The delineation of such ice hazard zones relies in part on the identification of geomorphic evidence such as bechevniks (Marusenko 1956; Hamelin 1979; Ettema 2002), bank erosion due to collapse of bankfast ice (Ettema 2002), fluvial gullies and scour holes (Smith & Pearce 2002), or ice scars on trees (Henoch 1973; Boucher *et al.* 2009). Confusion should not be made, however, between areas prone to river-ice run and areas that are prone to flooding because of ice jam floods, the latter areas being potentially much larger, although they are not entirely exposed to river-ice drifting. Additionally, distortion between water levels actually attained during ice jam floods and elevation of ice-run evidence such as tree scars can be important (Gerard 1981; Smith & Reynolds 1983).

This paper explores high accuracy mapping of inundations induced by ice jams in an Icelandic watershed. In the absence of the information required for deriving flood extent maps and flood depth maps from hydraulic modelling, photographs and aerial footage taken during recent ice jam floods were analysed. Along with on-site observations, archival documents such as aerial photographs taken during or soon after ice jam floods are well known to provide locally valuable information on the extent of breakup water levels (Kriwoken & Brown 1988). There is no indication, however, that imagery and DEMs at high resolution have already been used to support accurate reconstructions of historical ice jam floods based on the photo interpretation of aerial and ground photographs. The development, in recent years, of satellite imagery at sub-meter resolution (e.g. GeoEye-1, IKONOS) suggests that high accuracy reconstructions of ice jam floods could be performed on a large scale in the near future. In this case study, the water levels observed on the documents were identified on orthophotographs and georeferenced as control points in a Geographic Information System (GIS). They were finally attributed to corresponding elevation values observed in a DEM of 0.1 m vertical accuracy. The aim was to provide robust information on the extent and depth of flooding in the case of ice jam floods by analysing the differences of elevation between the topography and the irregular water surfaces resulting from the interpolation of the control points.

STUDY AREA

The Lower Reach of the Hvítá/Ölfusá hydrological complex was selected as a test area for the mapping at high accuracy of documented inundations induced by ice jam floods. The network pattern of the Ölfusá basin is controlled by tectonics and volcanism (Sigmundsson 2006; Thordarson & Hoskuldsson 2008); from Mount Hestfjall down to the Ölfusá estuary, the Hvítá/Ölfusá complex flows at the margin of the Great Þjórsá lava field (Hjartarson 1994), upon which the floodplain has developed (Figure 1): on the northern bank, the terrain slopes down to the river, while on the southern bank, the terrain slopes from the river down to the ocean at a mean rate of 0.13% (Figure 2). This nearly-flat area, partially altered into suitable terrains for farming during the 19th and 20th centuries, has been repeatedly flooded over the past 200 years because of ice jams that caused water encroachment and submersion of large areas that are safe from inundation under open-water conditions (Pagneux *et al.* 2010a). The boundaries and extent of such inundations depend essentially on the location and the nature of ice jams, irrespective of the discharge estimated at gauging sites.

Reliable flood mapping of the areas that are prone to ice jam floods cannot yet be achieved with hydraulic modelling as it requires information which is currently missing or inadequate:

- Although significant effort has been devoted in recent years to the densification of gauges in the lower reach, relevant upstream discharge information is missing for two-thirds of known ice jamming sites.

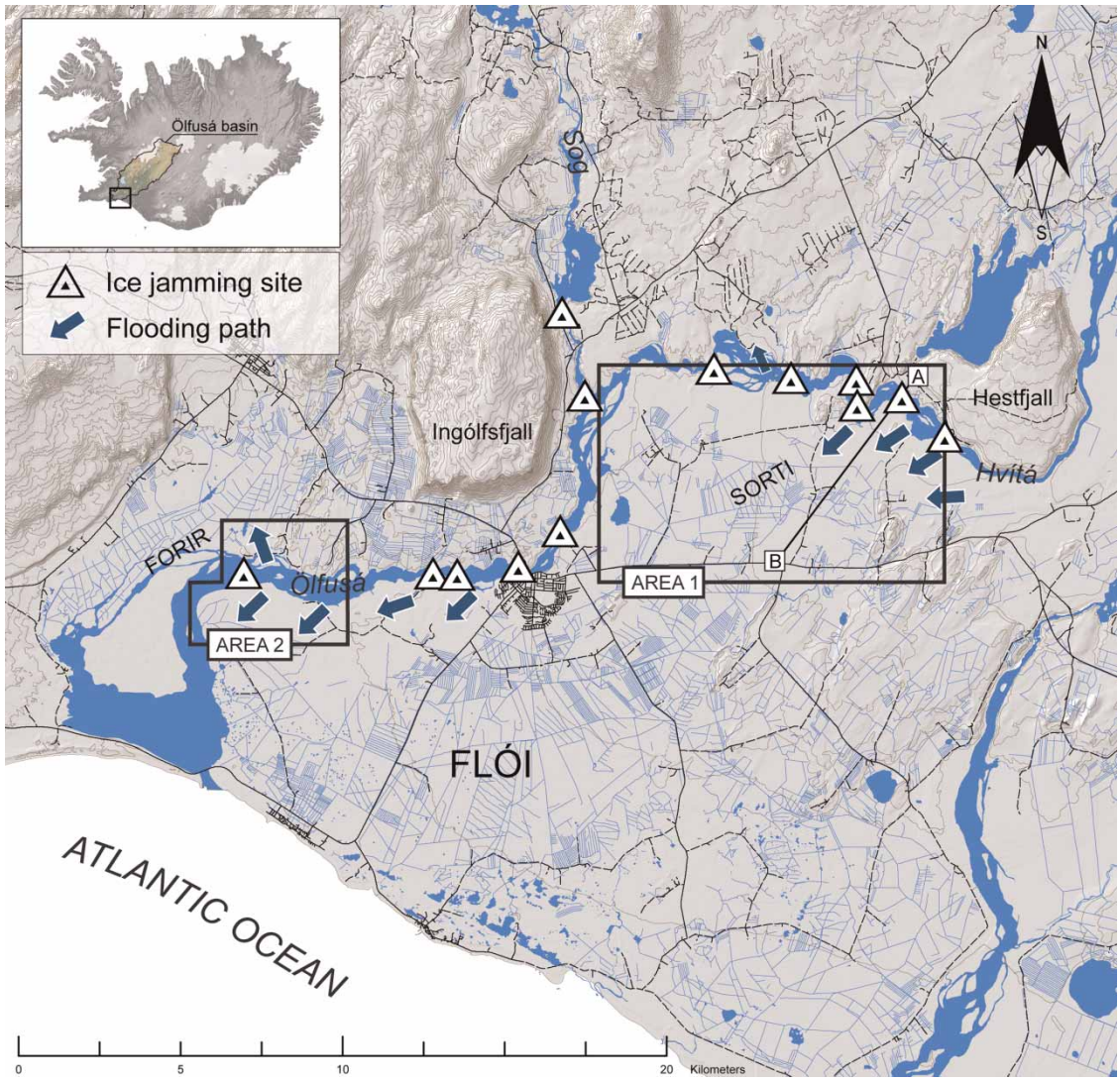

Figure 1 | Lower reach of the Ölfusá/Hvítá Rivers complex. Known ice jamming sites and associated flow paths active over the past 200 years (Pagneux *et al*. 2010a) are shown.

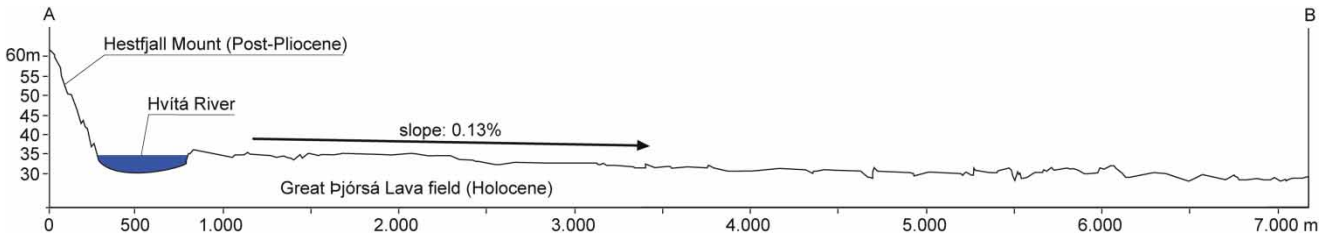

Figure 2 | Topographic transect from Mount Hestfjall (A) to Road 1 (B). Transect's location is shown in Figure 1; bathymetry of the Hvítá River is fictitious.

- Extensive information about the nature of ice jams involved is missing.
- The bathymetry of the Hvítá River and of the Ölfusá River remains unknown at most of the relevant sections.
- High permeability of the lava favours subsurface flow in areas where the Great Þjórsá lava field shows up at the surface; during river floods, hundreds of ponds can form on the lava outcrops and large areas behind

Table 4 | Ice jam flooding events selected for reconstruction. Rated 50-year flood, the reference historical flood for open-water conditions occurred on 21.12.2006, with a peak discharge of 1,840 m^3/s

Flooding event	Peak discharge at reference gauging site	Area	Place name	Documents	Control points created
14.1.2001	644 m^3/s	1	Sorti	12 aerial pictures, 4 ground pictures	267
23.1.1983	1,460 m^3/s	2	Kaldaðarnes/Arnarbæli	1 aerial footage,17 ground pictures	51

topographic obstacles can be flooded as water is dissipated through the lava.

The hydrogeomorphological approach, which derives delineation of flood envelope from the identification of active terraces and erosion forms (Lichvar *et al.* 2004; Ballais *et al.* 2005), brings some interesting information on areas that are prone to river-ice run. At the vicinity of some ice jamming sites, drifting river ice blocks have removed the histic and brown soil layers that cover most of the lower reach, and uncovered the Great Þjórsá lava field; soil removal is particularly obvious on aerial infrared imagery. Fluvial gullies can also be observed on holms at specific river sections. The absence of forests in the flood plain makes the delineation of ice hazard zones based on the identification of tree scars impossible (Boucher *et al.* 2009). At longer distances from the river, there is no more evidence of river ice scouring. Eventually, the photographs and footage showing past ice jam floods indicate that such ice hazard zones represent only a small fraction of the areas prone to inundation because of ice jam floods.

Methodology

Based on the simple analysis of elevation differences between water surfaces and topography (Priestnall *et al.* 2000), mapping of areas prone to ice jam floods relied on the photo interpretation of documented flooding events induced by ice jams. The photo interpretation of existing documents was supported with the use of orthophotographs and of a DEM of high vertical accuracy (±10 cm), which both originate from an airborne photogrammetric survey realised during the summer of 2008 from a mean altitude of 300 m above topography. Because of suspended glacial flour, the bathymetry of the Ölfusá River could not be estimated from the photogrammetric survey which only reflects the water levels observed during the flight. Two areas prone to ice jam floods were selected in the lower reach of the Hvítá/Ölfusá hydrological complex (Figure 1, Table 4). The selection was based on the availability of visual documents of good quality showing ice jam flooding events, and on the absence of severe modifications of the topography as the documented inundations occurred.

Data production and calculation

Multiple aerial and ground photographs of the flooding events, as well as footage from TV networks, were analysed. The water levels observed on the documents were identified on the orthophotographs, georeferenced as control points in a GIS, and eventually attributed elevation values according to the digital elevation model (Table 5). In some

Table 5 | Data production and calculation steps in ArcGis Desktop 9.3; extensions required are indicated

Steps	Description	Extension required
1	Creation of control points reflecting the water levels observed • Elevation values are attributed according to DTM	
2	Conversion of control points into irregular water surfaces (TINs) • Triangulation as mass points	3D Analyst
3	Conversion of terrain and irregular water surfaces into raster • Output Data Type: FLOAT • Method: LINEAR • Sampling distance: CELLSIZE 0.5 m	3D Analyst
4	Analysis of elevation differences (raster calculator) • Inundation extent = [Water raster] >= [Terrain raster] • Depth of flooding = [Water raster] – [Terrain raster]	Spatial Analyst
5	Conversion into polygons for manual corrections	

Table 6 | Definition of confidence indices reflecting reliability of reconstructions

Confidence index	Description
1 – High	Area mapped is entirely covered by visual documents. Number and density of control points reflecting water levels observed guaranty high accuracy of mapping
2 – Medium	Area mapped is not directly covered by visual documents. Distance between control points is too large to guaranty high accuracy of mapping

Table 7 | Reclassification of water depth based on safety and emergency response thresholds (MATE/METL 1999)

Thresholds	Description
0.5 m	Wading in water is unsafe for children
1 m	Buoyancy of vehicles; efficiency limit of individual water gates; wading in water is impossible for children, very difficult for elders
2.5 m	Upper limit of ground floor without construction level freeboard
4-class reclassification	**Gridcode**
Depth <0.5 m	1
0.5 m< depth <1 m	2
1 m< depth <2.5 m	3
Depth >2.5 m	4

circumstances, fictitious control points were created to allow a continuous calculation of the floodplain boundaries. The control points created were later converted into multiple triangular irregular networks (TIN), representing complex irregular water surfaces. Both the DEM and the irregular water surfaces created were then converted into raster images at 0.5 m resolution, to allow analyses of elevation differences with the raster calculator in ArcGis Desktop 9.3. Raster images obtained from the calculation process were ultimately converted into polygonal feature classes to allow manual corrections.

Product delivery

Because the available documents barely cover the whole extent of past flooding events, reconstruction at high resolution could not feature homogeneous levels of accuracy. The reconstructions were divided into regular cells of 1 km^2, each cell being applied a confidence index reflecting locally the reliability of reconstructions (Table 6). Deliverable to the general public and authorities, historical flood maps at scale 1:5000 were produced only for areas where the reconstructions were considered highly accurate. Originally obtained at a 10 cm contour interval, the depths of flooding were reclassified for legibility purpose on a four-class scale reflecting safety and emergency response thresholds (Table 7).

RESULTS AND DISCUSSION

Relying on the constitution of complex irregular surfaces, the reconstructions provide robust information on the boundaries and depth of flooding in case of ice jam floods (Figure 3) at a cost far inferior to the financial resources that should be allocated only to survey the river parameters required in hydraulic modelling. Information on bathymetry, discharge, friction values, and more importantly on the exact mechanics of ice jams involved, are not required. Only visual documents of good quality showing inundations induced by ice jam floods as well as orthophotographs and DEM at high resolution are needed, in a favourable context where identification of water levels is facilitated by the absence of forests.

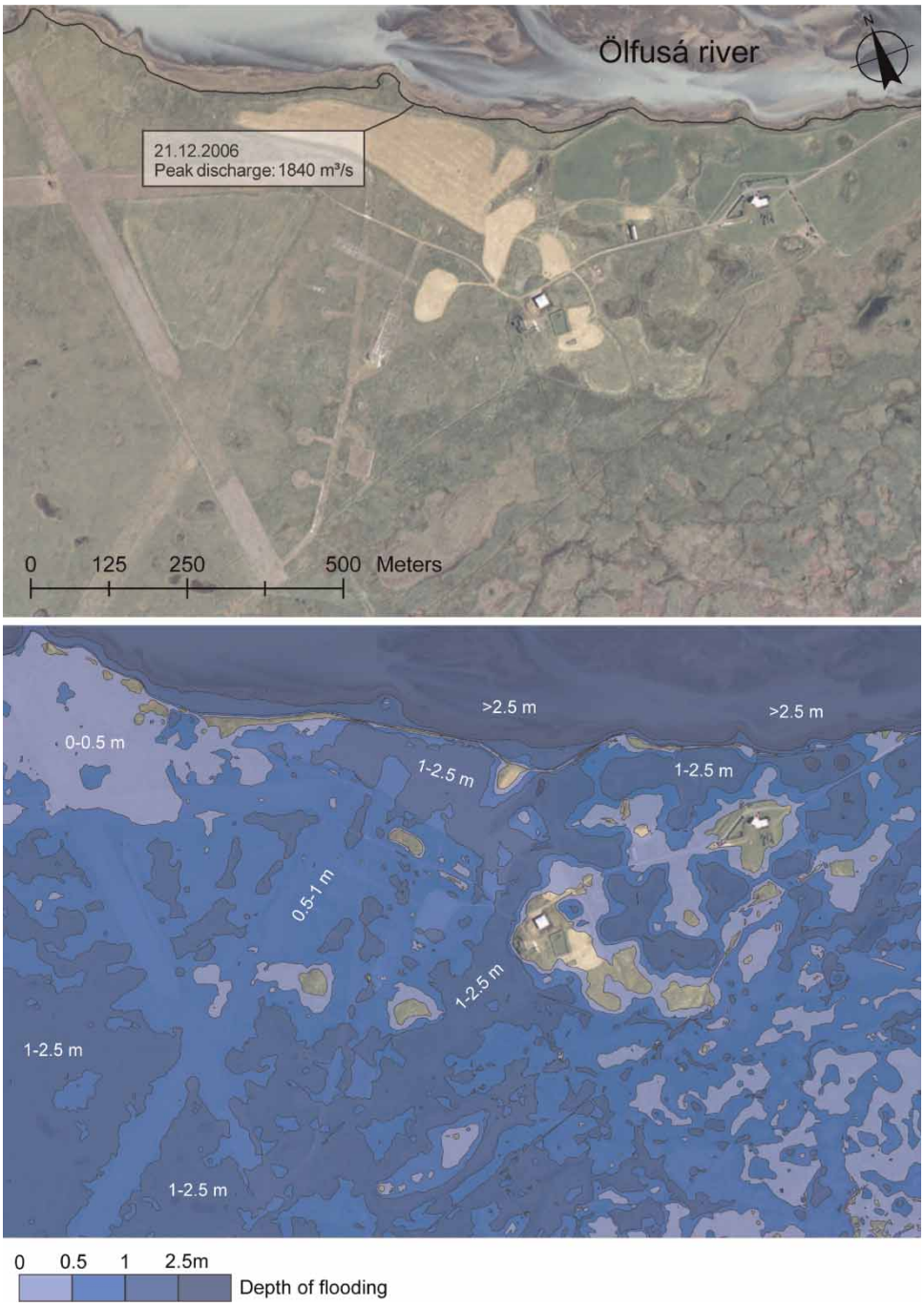

Figure 3 | Depth of flooding on 23.1.1983 by the farming estate of Kaldaðarnes (area 2 shown in Figure 1). Estimation is based on the photointerpretation of aerial footage and ground pictures. Boundary of the reference open-water flood, which occurred on 21.12.2006, is shown on the upper map for comparison. Orthophotograph: Samsýn ehf.© 2008.

From a theoretical perspective, the use of a documented flooding event as reference is, however, challenging. Because reconstructions do not rely on a probabilistic approach but on historical data, they provide information on flood hazard related to ice jam floods which cannot be considered as strictly predictive.

Some technical limitations are also challenging. Reliability of the documents is of course questionable with

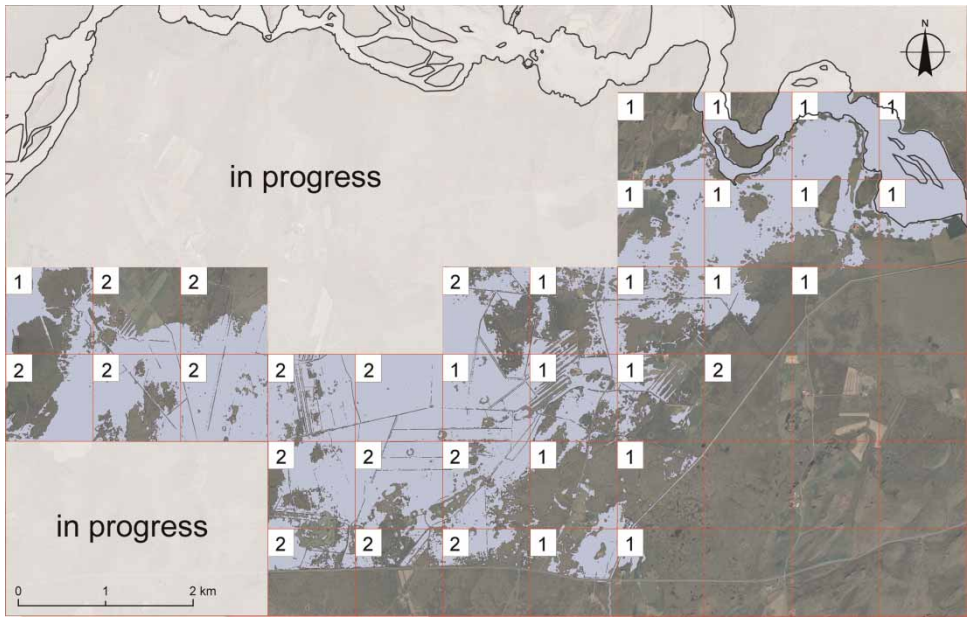

Figure 4 | Reconstruction of the flooding event on 14.1.2001 in area 1 (Figure 1). Boundaries of the Hvítá River are shown as dark lines. Confidence indices reflecting the reliability of the reconstruction (Table 6) are shown per cell of 1 km^2.

consideration of the timeline of flooding events. There is no guarantee that inundation boundaries obvious in the documents actually correspond to the highest water levels attained during the corresponding flooding events. Another important limitation comes from the fact that the material eligible to photo interpretation is often fragmentary for the reconstruction of past flooding events. Although information on boundaries and depth of flooding is robust in well-documented areas, the use of confidence indices is necessary when considering the whole extent of the flooding events reconstructed (Table 6; Figure 4). Some areas known to have been flooded in recent history (Pagneux *et al.* 2010a) could not be mapped at high resolution because of the lack of observable water levels. The use of imagery from sub-meters satellites could ensure high accuracy on a large scale to reconstructions of future events. Imagery from the sub-meter satellite IKONOS (Dial *et al.* 2003) has been used, for instance, by the Icelandic Meteorological Office to complete boundary mapping of the glacial bursts triggered on 14–15 April 2010 by the eruption of Eyjafjallajökull Volcano. Limitations due to the fragmentation of documents and the absence of flood routing may thus be overcome in the future.

The cleaning phase, which partly consists in the deletion of polygons, may also be problematic in areas prone to hypodermic or subsurface flows. This is especially the case in areas where the postglacial Great Þjórsá lava field shows up at the surface. Also an issue for hydraulic modelling, subsurface flow makes the use of aerial survey indispensable.

Unlike storage cell models, e.g. LISFLOOD-FP (Bates & de Roo 2000), and 1D–2D hydraulic models, the reconstructions of past flooding events according to photo interpretation do not include flood routing formulae; estimation of the extent and depth of flooding events only relies on the analyses of elevation differences between the topography and the irregular water surfaces created. The reconstructions, therefore, require extra caution when placing and selecting the control points in the interpolation process; a great number of control points may be necessary when the topography is complex and flow multi-channelised.

An ultimate limitation comes from the fact that one area can be flooded from different encroachment sites (Figure 1), each having a specific impact on the extent, boundaries and depth of flooding events (Pagneux *et al.* 2010a). Unfortunately, ice jam floods in the lower reach of the Ölfusá River that are documented with photographs and footage refer only to one-fifth of known ice jamming sites.

Despite limitations inherent in the methodology, reconstructions provide locally unprecedented information on the

boundaries and depth of flooding in case of ice jam floods. Because ice jam floods are extreme events in comparison to open-water floods, the reconstructions should be regarded as providing essential information for a danger-oriented classification of areas prone to floods liable to be used for planning purpose as well as for emergency response; in the absence of information about flow velocity, such a classification could rely on water depth thresholds only (MATE/METL 1999). Regarding the assessment of flood hazard, the reconstructions should be useful for the calibration of hydraulic models in the assessment of ice jams floods once the river bathymetry and the nature of ice jams are known and a relevant discharge estimated upstream. They may be also used with field and remote sensing data for the calibration of hydraulic models for open-water floods.

CONCLUSION

The use of orthorectified imagery and a high resolution DEM allows accurate reconstruction of past ice jam floods that are still of relevance and are consistently documented with archives including aerial and ground photographs. Although not being strictly predictive, robust information on the boundaries and water depth of inundations induced by ice jam floods is provided locally; as depth of flooding is a crucial parameter, considerable weight is hence given to historical approaches in the assessment of flood hazard and in the management of flood risk. Tested in an Icelandic watershed where topographic conditions are admittedly difficult, such an approach could be of interest in cold-climate regions prone to ice jam floods, when information necessary for the use of hydraulic models is lacking and financial resources limited.

ACKNOWLEDGEMENTS

This work was financially supported by Rannís – the Icelandic Centre for Research (Research Grant # 080071/5264). We would like to thank Bogi B. Björnsson and Matthew J. Roberts from the Icelandic Meteorological Office for their assistance and the reviewers for their helpful and constructive comments. We are grateful to Lýður Pálsson and Jón Eiriksson for their generous contribution to ground pictures collection.

REFERENCES

Bales, J. D., Wagner, C. R., Tighe, K. C. & Terziotti, S. 2007 *LiDAR-Derived Flood-Inundation Maps for Real-Time Flood-Mapping Applications, Tar River Basin, North Carolina*. US Department of the Interior, US Geological Survey, Scientific Investigations Report 2007-5032.

Bales, J. D. & Wagner, C. R. 2009 Sources of uncertainty in flood inundation maps. *J. Flood Risk Manage.* **2**, 139–147.

Bates, P. D. & de Roo, A. P. J. 2000 A simple raster-based model for flood inundation simulation. *J. Hydrol.* **236**, 54–77.

Ballais, J. L., Garry, G. & Masson, M. 2005 Contribution de l'hydrogéomorphologie à l'évaluation du risque d'inondation: le cas du Midi méditerranéen français. *C.R. Geosci.* **337**, 1120–1130 (in French).

Beltaos, S. 1995 Ice jam processes. In: *River Ice Jams* (S. Beltaos, ed.). Water Resources Publications, Highlands Ranch, CO, USA pp. 71–104.

Beltaos, S. 2008 Progress in the study and management of river ice jams. *Cold Regions Sci. Technol.* **51**, 2–19.

Boucher, E., Bégin, Y. & Arseneault, D. 2009 Impacts of recurring ice jams on channel geometry and geomorphology in a small high-boreal watershed. *Geomorphology* **108**, 273–281.

Carson, R. W., Beltaos, S., Healy, D. & Groeneveld, J. 2003 Tests of river ice jam models – Phase 2. 12th Workshop on the Hydraulics of Ice Covered Rivers, CGU-HS Committee on River Ice Processes and the Environment. Canada, Edmonton, June 19–20 2003, pp. 291–305.

Department of Communities and Local Government (DCLG) 2006 *Planning Policy Statement 25: Development and Flood Risk*. The Stationery Office, Norwichm UK.

DEFRA 2006 *Flood Risk to People. Phase 2*. FD2321/TR2 Guidance document. Environment Agency and Department for Environment, Food and Rural Affairs Location, London, UK. Available from: http://www.rpaltd.co.uk/documents/J429-RiskstoPeoplePh2-Guidance.pdf.

DEFRA 2008 Supplementary note on flood hazard ratings and thresholds for development planning and control purpose. Clarification of the Table 13.1 of FD2320/TR2 and Figure 3.2. of FD2321/TR1.

de Moel, H., van Alphen, J. & Aerts, J. C. J. H. 2009 Flood maps in Europe – methods, availability and use. *Nat. Hazards Earth Syst. Sci.* **9**, 289–301.

Dial, G., Bowen, H., Gerlach, F., Grodecki, J. & Oleszczuk, R. 2003 IKONOS satellite, imagery, and products. *Remote Sens. Environ.* **88**, 23–36.

Environment Canada 1993 *Flooding: Canada Water Book*. Economics and Conservation Branch, Ecosystem Sciences and Evaluation Directorate, Environment Canada, Ottawa.

Ettema, R. 2002 Review of alluvial-channel responses to river ice. *J. Cold Regions Eng.* **16** (4), 191–217.

European Parliament, Council 2007 Directive 2007/60/EC of the European Parliament and of the Council of 23 October 2007 on the assessment and management of flood risks. *Official J. Lett. 288* 6.11.2007, 27–34.

EXCIMAP 2007 *Handbook on Good Practices for Flood Mapping in Europe* (F. Martini & R. Loat R, eds). The Netherlands Ministry of Transport, Public Works and Water Management, The Hague, 197 pp. Available from: http://ec.europa.eu/environment/water/floodrisk/floodatlas/index.htm.

French Parliament 1995 Loi n° 95-101 du 2 février 1995 relative au renforcement de la protection de l'environnement. *JORF* **29**, 3.02.1995, pp. 1840–1856 (in French).

Gerard, R. 1981 Ice scars: are they reliable indicators of past ice breakup water levels? Proc. Int. Symp. on Ice, IAHR, Québec, Canada, July 27–31 1981, pp. 847–854.

Government of Alberta, Flood hazard mapping – Alberta Environment, available from: http://environment.alberta.ca/01655.html.

Government of Alberta, Flood Damage Reduction Program, available from: http://www3.gov.ab.ca/env/water/flood/FDRP.pdf.

Hamelin, L. E. 1979 The bechevnik: a river bank feature from Siberia. *Musk Ox* **25**, 70–72.

Henoch, W. E. S. 1973 Data on height, frequency of floods, ice jamming, and climate from tree-ring studies. In: *Hydrologic Aspects of Northern Pipeline Development* (D. K. MacKay, ed.). Information Canada Report, Information Canada, Ottawa, pp. 157–177.

Hjartarson, Á. 1994 Environmental changes in Iceland following the great Thjórsá lava eruption 7800 ^{14}C years BP. In: *Environmental Change in Iceland* (J. Stötter & F. Wilhelm, eds). Münchener Geographische Abhandlungen B12, München, pp. 147–155.

Horrit, M. S., Bates, P. D., Fewtrell, T. J. & Mason, D. C. 2010 Modelling the hydraulics of the Carlisle 2005 flood event. *Proc. Inst. Civil Engs., Water Management* **163**, 273–281.

Kelman, I. & Spence, R. 2004 An overview of flood actions on buildings. *Eng. Geol.* **73**, 293–309.

Kreibich, H., Piroth, K., Seifert, I., Maiwald, H., Kunnert, U., Schwarz, J., Merz, B. & Thieken, A.H. 2009 Is flow velocity a significant parameter in flood damage modelling? *Nat. Hazards Earth Syst. Sci.* **9**, 1679–1692.

Kriwoken, L. A. & Brown, D. W. 1988 Using historical data to determine flood risk from ice jams. 5th Workshop on Hydraulics of River Ice/Ice Jams, 21–24 June 1988, Winnipeg, Manitoba.

Lichvar, R., Finnegan, D. C. & Ericsson, M. P. 2004 Using hydrogeomorphic surfaces for delineating floodplains: Black Water Creek Test reach within the Upper Puerco watershed, Navajo nation. ERDC/CRREL Technical note 04-7.

Liu, L., Li, H. & Shen, H. T. 2006 A two-dimensional comprehensive river ice model. Proceedings of the 18th International Symposium on Ice, IAHR, Aug. 28–Sept. 1, pp. 69–76.

Marusenko, Y. I. 1956 Ice action on river banks. *Priroda* **12**, 91–93.

MATE/METL 1999 Plans de Prévention des Risques Naturels (PPR): Risques d'inondation. Guide méthodologique. Ministère de l'Aménagement du Territoire et de l'Environnement & Ministère de l'Equipement, des Transports et du Logement, La Documentation Française, Paris (in French).

Merz, R., Blöschl, G. & Humer, G. 2008 National flood discharge mapping in Austria. *Nat Hazards* **46**, 53–72.

Moyeed, R. A. & Clarke, R. T. 2005 The use of Bayesian methods for fitting rating curves, with case studies. *Adv. Water Res.* **28** (8), 807–818.

NARA 2009 Flood plain Management and protection of wetlands. *US Code of Federal Regulations*, Title 44, part 9, Chapter 1, vol. 1. pp. 69–88.

Pagneux, E., Gísladóttir, G. & Snorrason, Á. 2010 Inundation extent as a key parameter for assessing the magnitude and return period of flooding events in South Iceland. *Hydrol. Sci. J.* **55** (5), 704–716.

Priestnall, G., Jaafar, J. & Duncan, A. 2000 Extracting urban features from LiDAR digital surface models. *Computers Environ. Urban Syst.* **24** (2), 65–78.

Sigmundsson, F. 2006 *Iceland Geodynamics: Crustal Deformation and Divergent Plate Tectonics*. Praxis Publishing, Springer, Chichester, UK.

Smith, D. G. & Reynolds, D. M. 1983 Tree scars to determine the frequency and stage of high magnitude river ice drives and jams, Red Deer, Alberta. *Can. Water Res. J.* **8** (3), 77–94.

Smith, D. G. & Pearce, C. M. 2002 Ice jam-caused gullies and scour holes on northern river flood plains. *Geomorphology* **42**, 85–95.

Spachinger, K., Dorner, W., Metzka, R., Serrhini, K. & Fuchs, S. 2008 Flood Risk and Flood Hazard Maps – Visualisation of Hydrological Risks. *IOP Conf. Ser.: Earth Environ. Sci.* **4**, 012043.

Thordarson, T. & Hoskuldsson, A. 2008 Post glacial volcanism in Iceland. *Jökull* **58**, 197–227.

First received 22 November 2010; accepted in revised form 4 May 2011. Available online 27 January 2012